Robust Backstepping Sliding Mode Control and Observer-Based Fault Estimation for a Quadrotor UAV

Fuyang Chen, Rongqiang Jiang, Kangkang Zhang, Bin Jiang, *Senior Member*, *IEEE*, and Gang Tao, *Fellow*, *IEEE*

***Abstract*—This study gives the mathematic model of a quadrotor unmanned aerial vehicle (UAV) and then proposes a robust nonlinear controller which combines the sliding mode control technique and the backstepping control technique. To achieve Cartesian position trajectory tracking capability, the construction of the controller can be divided into two stages: a regular SMC controller for attitude subsystem (inner loop) is first developed to guarantee fast convergence rapidity of Euler angles and the backstepping technique is applied to the position loop until desired attitudes are obtained and then the ultimate control laws. The stability of the closed-loop system is guaranteed by stabilizing each of the subsystems step by step and the robustness of the controller against model uncertainty and external disturbances is investigated. In addition, an adaptive observer-based fault estimation scheme is also considered for taking off mode. Simulations are conducted to demonstrate the effectiveness of the designed robust nonlinear controller and the fault estimation scheme.**

***Index Terms*—Backstepping control, Sliding mode control, Quadrotor UAV, Robustness, Fault estimation**

I. INTRODUCTION

AS a new-born member of the small unmanned aerial vehicle (UAV) family, quadrotor is becoming a popular topic among researchers and scholars because of its extensive utility in several important applications such as military surveillance, disaster monitoring, agricultural mapping, and rescue mission and so on [1]. The main advantages of quadrotor UAVs lie in flying in any direction, taking off and landing vertically and hovering at a desired altitude. However, its characteristics, such as nonlinearity, strong coupling and under-actuating, make designing an effective controller for position trajectory tracking control difficult. What's more, taking robustness of the trajectory tracking controller into consideration poses a bigger challenge.

In the past few years, researchers have paid attention to control and have proposed different kinds of control methods, such as linear and adaptive PID controls [2-3], dynamic inversion Control [4], feedback linearization control [5-6], model predictive control [7], backstepping control [8-9], sliding mode control (SMC) [10-11], LMI-based linear control [12], observer-based control [13-18], adaptive control [19-21] and nonlinear control [22-23], just to numerate a few. Recently, with the development of intelligence control theory, some advanced or modified controllers, which combine the aforementioned basic methods with intelligent control methods, such as fuzzy control and switching topology, have been presented for a few complicated tasks [24-26]. Fault tolerant control and robust control methods are also becoming much more popular for fault tolerance and robustness against disturbances, respectively [20, 27-31]. The performances of these controllers are satisfying in terms of attitude or position trajectory tracking capability when some particular circumstances are considered. For instance, [1] proposed a new feedback control scheme for attitude stabilization of a quadrotor; [2] designed a flight control system capable of not only stabilizing attitude but also tracking a trajectory accurately for an under-actuated quadrotor aircraft; [18] presented a robust attitude tracking controller for quadrotors based on the nonlinear disturbance observer; [29] proposed a robust controller consist of a nominal feedforward controller, a nominal linear LQR controller and a robust compensator to deal with robust attitude control problem. The proposed controllers aforementioned are demonstrated to be effective in some specific cases. However, all the works above are limited to attitude trajectory tracking control problem and lack focus on position control which has highly important practical utilities. On the other hand, many existing works that aimed at position trajectory tracking control have either paid little attention to robustness and fault tolerance of the proposed controllers or preferred a simplified form of dynamic equation, for example, [6] presented a feedback linearization controller and noticed its sensitivity to noise and modeling uncertainly, so further presented a sliding mode controller to overcome it, however, the quadrotor dynamics is a simplified one and the coupling between attitudes and positions was omitted; [9] applied backstepping

Manuscript received April 5, 2015; revised August 8, 2015 and November 18, 2015; accepted December 22, 2015. The project was supported by the Aeronautics Science Foundation of China (2014ZC52033) and the National Natural Science Foundation of China (61533009, 61473146, 61374130), a project funded by the Priority Academic Programme Development of Jiangsu Higher Education Institutions.

F. Chen, R. Jiang, K. Zhang and B. Jiang are with the College of Automation Engineering, Nanjing University of Aeronautics and Astronautics, Nanjing 210016, China (e-mail: chenfuyang@nuaa.edu.cn; jrongqiang @163.com; kkzhangnuaa@163.com; binjiang@nuaa.edu.cn).

G. Tao is with the Department of Electrical and Computer Engineering, University of Virginia, Charlottesville, VA 22903, USA (e-mail: gt9s@virginia.edu).

control on the Lagrangian form of the dynamics of a quadrotor and also adopted a simplified form of dynamics; [23] presented a nonlinear adaptive state feedback controller that stabilizes the closed-loop system in the presence of force disturbances, however, the adopted model was a nominal one and the disturbance was assumed to be constant which is often not the case. Motivated by these, this study investigates the possibility of a robust backstepping sliding mode controller for the nonlinear strong coupled model of a quadrotor UAV.

As an extensively used nonlinear control method, SMC features excellent performance properties and robustness for a specific class of nonlinear tracking problems [32-33] and is also used in some areas to address practical and important issues [36-38]. SMC utilizes a high frequency switching control signal to enforce the system trajectories onto a surface, that is, the so-called sliding surface or sliding manifold which is designed to achieve desired specifications. In a finite time, the system trajectories arrive and remain within the vicinity of the sliding surface. The sliding mode control is robust with respect to internal and external disturbances, as well as parameter uncertainties which accounts for its popularity among the nonlinear control methods. Quadrotor position control is a typical nonlinear control problem because complicated nonlinearity and coupling exist in its dynamics. And further, researchers have developed some improved sliding mode controllers with robustness against perturbation and uncertainties [10, 27]. However, most of the existing literatures have focused on using SMC methods to address attitude control of a quadrotor UAV rather than position trajectory tracking control design since the transformed dynamics equation has a preferable form for attitude control. However, position control has highly important practical utilities and correspondingly increased difficulties in control design.

Backstepping technique starts the control design process in feedback form at the origin of a complicated system and backs out to new controllers that stabilize each outer subsystem step by step. Virtual controls are utilized in these steps to guarantee the stability of each subsystem and they are finally determined by performance specifications. The backing out process continues until the ultimate control law is obtained. However, in many existing research works, backstepping control is utilized alone for position control of a quadrotor UAV with very little discussion about robustness against external disturbances and model uncertainties [8]. In this study, we consider a position trajectory tracking control for a quadrotor UAV with the consideration of robustness against disturbances and model uncertainties. As the study will show, we combine the SMC and the backstepping control techniques to develop a robust backstepping sliding mode controller which is constructed by two stages. A regular sliding mode controller for attitude control is first designed to guarantee fast attitude trajectory tracking capability. Then, we use backstepping technique for Cartesian position trajectory tracking control and obtain a group of equations by mathematically solving which the desired Euler angles are given. Applying the desired angles as input for the attitude system, the final robust sliding mode control laws are then developed. In constructing the robust nonlinear controller, "virtual control" and sliding manifold are used to guarantee position trajectory tracking capability as well as robustness against disturbances and uncertainties.

Compared with traditional aircrafts, a quadrotor UAV is more likely to encounter problems such as actuator faults, which threaten the system's stability and reliability. These potential problems pose a challenge to the applications of a quadrotor UAV in some significant situations [34]. A lot of work has been done in fault diagnosis field. In the past few years, model-dependent methods have been studied and mature [35]. Recently, new data-driven methods are being been researched and some results have been produced [38-41]. Inspired by the methods applied to handle conventional fixed-wing aircraft's actuator faults, fault tolerant control is a possible option for a quadrotor UAV. The key issue for fault tolerant control rests with obtaining enough information about faults where the fault estimation scheme plays an important role. Thus, apart from robust controller design, fault estimation scheme is also considered in some certain cases to supplement the controller design.

This paper is organized as follows. A non-simplified mathematic model is first developed. Afterwards, a sliding mode controller for attitude trajectory control is presented, followed by a robust backstepping sliding mode controller for position trajectory tracking control. In addition, an observer-based fault estimation scheme is considered and the conditions and constraints for its applicability are provided. Simulations are conducted in different scenarios to demonstrate the effectiveness of the proposed robust backstepping sliding mode controller and the fault estimation scheme. Conclusions are drawn in the end of this paper.

II. DYNAMIC MODEL

Quadrotor is an under-actuated system because it has six degrees of freedom but only four actual inputs. The six degrees of freedom include translational motion in three directions and rotational motion around three axes. The schematic configuration of a quadrotor we adopted in this study is shown in Fig.1. Four rotors, each of which is driven by a motor, are mounted at two orthogonal directions and rotates in a direction as the circular arrow shows. The body-fixed frame which is represented by $Ox_by_bz_b$ with its origin at the center of the mass and the inertia frame which is represented by $Ox_ey_ez_e$ are as shown in Fig.1. The front (Rotor 1) and the rear (Rotor 3) rotors rotate counter clockwise, while the lateral rotors (Rotor 2 and Rotor 4) rotate clockwise to generate the lift force and to balance the yaw torque as needed. On varying the rotor speeds altogether with the same quantity, the lift forces will change, affecting the altitude of the vehicle in this case. Pitch rotation can be obtained by changing the speeds of the front and the rear rotors conversely while coupled with translation along Ox_b. Roll rotation and translation along Oy_b can be obtained in a similar way by varying the speeds of the lateral ones conversely. The equations describing the dynamics of a quadrotor are basically those of a rotating rigid body with six degrees of freedom which can be derived with Newton-Euler formulas. The complicated motions of a quadrotor can be described by two typical groups of equations, each of which represents a subsystem with coupled terms. The first group is related to the translational positions and the second group is related to the rotational angles. In this section, we will give the quadrotor UAV's mathematic model including the navigation equations and the moment equations [1].

This article has been accepted for publication in a future issue of this journal, but has not been fully edited. Content may change prior to final publication. Citation information: DOI 10.1109/TIE.2016.2552151, IEEE Transactions on Industrial Electronics

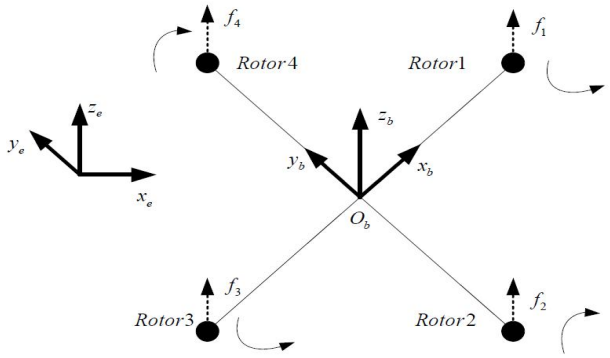

Fig.1 Quadrotor configuration frame scheme with body fixed and the inertia frames

Define $\xi=[\phi,\theta,\psi]^T\in\Re^3$ and $\omega_b=[p,q,r]^T$, where ϕ, θ and ψ denote the angle of roll, pitch and yaw with respect to the inertia frame and p, q and r denote the angular velocity of roll, pitch and yaw with respect to the body-fixed frame. The rotation matrix from body-fixed frame to inertia frame can be obtained as:

$$R_t=\begin{bmatrix} C_\psi C_\theta & C_\psi S_\theta S_\phi - S_\psi C_\phi & C_\psi S_\theta C_\phi + S_\psi S_\phi \\ S_\psi C_\theta & S_\psi S_\theta S_\phi + C_\psi C_\phi & S_\psi S_\theta C_\phi - C_\psi S_\phi \\ -S_\theta & C_\theta S_\phi & C_\theta C_\phi \end{bmatrix} \tag{1a}$$

where $S_{(\cdot)}$ and $C_{(\cdot)}$ denote $\sin(\cdot)$ and $\cos(\cdot)$ respectively In particular, R_t is an orthogonal matrix which means that $R_t^T=R_t^{-1}$ when R_t is nonsingular. In particular, the transformation matrix R_t mentioned in (1a) is special because the following equation holds

$$\dot{R}_t=R_tS(\omega_b) \tag{1b}$$

where $S(\omega_b)$ is a skew symmetric matrix which means $S^T(\omega_b)=-S(\omega_b)$ and $S(\omega_b)$ is given as:

$$S(\omega_b)=\begin{bmatrix} 0 & -r & q \\ r & 0 & -p \\ -q & p & 0 \end{bmatrix} \tag{1c}$$

For any given $V=[v_1 \quad v_2 \quad v_3]^T\in\Re^3$, it is easy to verify

$$S(\omega_b)\cdot V=\omega_b\times V \tag{2a}$$

According to the rotation matrix R_t the relationship between $\dot{\xi}$ and ω_b can be described as:

$$\omega_b=R_r\dot{\xi}=\begin{bmatrix} 1 & 0 & -S_\theta \\ 0 & C_\phi & C_\theta S_\phi \\ 0 & -S_\phi & C_\theta C_\phi \end{bmatrix}\begin{pmatrix} \dot{\phi} \\ \dot{\theta} \\ \dot{\psi} \end{pmatrix} \tag{2b}$$

M_b is defined as the torque provided by the rotors with respect to the body-fixed frame, and is described as follows:

$$M_b=\begin{bmatrix} M_{bx} \\ M_{by} \\ M_{bz} \end{bmatrix}=\begin{bmatrix} l\kappa(\Omega_4^{\,2}-\Omega_2^{\,2}) \\ l\kappa(\Omega_3^{\,2}-\Omega_1^{\,2}) \\ \tau(\Omega_2^{\,2}+\Omega_4^{\,2}-\Omega_1^{\,2}-\Omega_3^{\,2}) \end{bmatrix} \tag{3a}$$

where Ω_i, $i=1,2,3,4$ denote rotary speed of the front, right, rear, and left rotors, respectively; l is the distance between a rotor and the center of mass of the quadrotor; κ is the drag force coefficient; and τ is reverse moment coefficient.

Using the Newton–Euler equation, the rotational dynamic equation of the quadrotor is obtained as follows:

$$M_b=J_b\dot{\omega}_b+\omega_b\times J_b\omega_b+M_g+M_d \tag{3b}$$

where $J_b=diag(J_x,J_y,J_z)$ is a symmetric positive definite constant matrix with J_x, J_y and J_z being the rotary inertia with respect to the O_bx_b, O_by_b, and O_bz_b axes, respectively; the notation $\times$ denotes cross multiplication; M_g and M_d are the resultant torques due to the gyroscopic effects and the resultant of aerodynamic frictions torque. They are given as:

$$\begin{aligned} M_g&=\sum_{i=1}^{4}\omega_b\times J_r\left[0,\ 0,\ (-1)^{i+1}\Omega_i\right]^T \\ M_d&=diag(\mathrm{d}_\phi,\mathrm{d}_\theta,\mathrm{d}_\psi)\dot{\xi}^2 \end{aligned} \tag{3c}$$

where J_r is the moment of inertia of each rotor; d_ϕ, d_θ and d_ψ are the corresponding aerodynamic drag coefficients.

Considering that J_b is nonsingular and transforming (3b), the following equation can be obtained:

$$\dot{\omega}_b=J_b^{-1}\left[M_b-M_g-M_d-\omega_b\times(J_b\omega_b)\right] \tag{4}$$

Furthermore, with the aid of (1c), (2a)-(2b) and approximation of Euler angles at equilibrium point, the following dynamic equations can be obtained:

$$\begin{aligned} \ddot{\phi}&=(\dot{\theta}\dot{\psi}(J_y-J_z)-J_r\dot{\theta}\varpi-d_\phi\dot{\phi}+M_{bx})/J_x \\ \ddot{\theta}&=(\dot{\phi}\dot{\psi}(J_z-J_x)-J_r\dot{\phi}\varpi-d_\theta\dot{\theta}+M_{by})/J_y \\ \ddot{\psi}&=(\dot{\phi}\dot{\theta}(J_x-J_y)-d_\psi\dot{\psi}+M_{bz})/J_z \end{aligned} \tag{5}$$

where $\varpi=\Omega_4+\Omega_3-\Omega_2-\Omega_1$ can be obtained easily online.

Remark 2.1: It is worth nothing to point out that the roll and pitch angles are limited to $(-\pi/2,\pi/2)$ which is physically meaningful. In particular, the yaw angle in this study is also limited to $(-\pi/2,\pi/2)$.

Let $P=[x,y,z]^T\in\Re^3$ denote the position with respect to the inertia frame. The translational dynamic equations of the quadrotor is given by

$$m\ddot{P}=R_t\cdot F+\begin{bmatrix} 0 \\ 0 \\ -mg \end{bmatrix}-\begin{bmatrix} d_x\dot{x} \\ d_y\dot{y} \\ d_z\dot{z} \end{bmatrix} \tag{6}$$

where R_t is given in (1a), and d_x, d_y and d_z are the air drag coefficients which are added in (6) to model the drag force caused by translational motions; F is the lift force generated by rotors with respect to the body-fixed frame

$$F=\begin{bmatrix} 0 \\ 0 \\ \kappa(\Omega_1^{\,2}+\Omega_2^{\,2}+\Omega_3^{\,2}+\Omega_4^{\,2}) \end{bmatrix} \tag{7}$$

By combining (5) and (6), a compact affine nonlinear equation of the quadrotor UAV is given

$$\dot{X}=f(X)+g(X)U \tag{8}$$

where $X=[\phi,\dot{\phi},\theta,\dot{\theta},\psi,\dot{\psi},x,\dot{x},y,\dot{y},z,\dot{z}]^T\in\Re^{12}$ is the state variable, $f(X)$ and $g(X)$ are smooth functions on X. The Equation (8) is expended as follows:

$$\begin{cases} \dot{x}_1 = x_2 \\ \dot{x}_2 = a_1 x_4 x_6 + a_2 \varpi x_4 - a_3 x_2 + U_1 \\ \dot{x}_3 = x_4 \\ \dot{x}_4 = a_4 x_2 x_6 + a_5 \varpi x_2 - a_6 x_4 + U_2 \\ \dot{x}_5 = x_6 \\ \dot{x}_6 = a_7 x_2 x_4 - a_8 x_6 + U_3 \\ \dot{x}_7 = x_8 \\ \dot{x}_8 = (C_{x_1} S_{x_3} C_{x_5} + S_{x_1} S_{x_5}) U_4 - a_9 x_8 \\ \dot{x}_9 = x_{10} \\ \dot{x}_{10} = (C_{x_1} S_{x_3} S_{x_5} - S_{x_1} S_{x_5}) U_4 - a_{10} x_{10} \\ \dot{x}_{11} = x_{12} \\ \dot{x}_{12} = -g + (C_{x_1} C_{x_3}) U_4 - a_{11} x_{12} \end{cases} \tag{9}$$

where ϖ, d_ϕ, d_θ, d_ψ, l, κ, $C_{(\cdot)}$, $S_{(\cdot)}$ and m are same as those mentioned earlier and g is the gravity acceleration. U_i, $i = 1,2,3,4$ are the control inputs defined as follows:

$$\begin{aligned} U_1 &= l\kappa(\Omega_4{}^2 - \Omega_2{}^2)/J_x \\ U_2 &= l\kappa(\Omega_3{}^2 - \Omega_1{}^2)/J_y \\ U_3 &= l\kappa(\Omega_4{}^2 + \Omega_2{}^2 - \Omega_3{}^2 - \Omega_1{}^2)/J_z \\ U_4 &= l\kappa(\Omega_1{}^2 + \Omega_2{}^2 + \Omega_3{}^2 + \Omega_4{}^2)/m \end{aligned} \tag{10}$$

and a_i, $i = 1,2,\cdots 11$, are the normalized parameters defined as follows:

$$a_1 = \frac{J_y - J_z}{J_x},\ a_2 = \frac{J_r}{J_x},\ a_3 = \frac{d_\phi}{J_x},\ a_4 = \frac{J_z - J_x}{J_y},\ a_5 = \frac{J_r}{J_y},$$

$$a_6 = \frac{d_\theta}{J_y},\ a_7 = \frac{J_x - J_y}{J_z},\ a_8 = \frac{d_\psi}{J_z},\ a_9 = \frac{d_x}{m},\ a_{10} = \frac{d_y}{m},\ a_{11} = \frac{d_z}{m}.$$

III. BACKSTEPPING SLIDNG MODE CONTROLLER FOR POSITIOIN TRAJECTORY TRACKING CONTROL

In this section, a regular sliding mode controller for attitude trajectory tracking control is first presented. The SMC technique is then combined with the backstepping control technique to develop a robust backstepping sliding mode controller for position trajectory tracking control. The regular sliding mode controller is designed to ensure the trajectory tracking capability of $\{\phi(t),\theta(t)\}$ along the desired roll and pitch angle trajectory $\{\phi_d(t),\theta_d(t)\}$. The robust backstepping sliding mode controller constructed based on the regular controller aims to ensure the position and yaw angle tracking performance along the reference input $\{x_r(t), y_r(t), z_r(t), \psi_r(t)\}$ robustly. The block diagram of control structure is shown in Fig.2.

A. Regular Sliding Mode Controller for Attitude Trajectory Tracking Control

The sliding mode control features acceptable robustness in the presence of model uncertainties and external disturbances for a specific class of nonlinear tracking problems and becomes a good choice for attitude control of a quadrotor UAV. SMC focuses on designing a sliding manifold and discontinuous control laws that drive the system toward the desired dynamic behavior and ensure the tracking performance. This kind of direct nonlinear control strategy for a complicated coupled nonlinear system avoids the inaccuracy caused by linearization around the operation points, and is extensively applied in nonlinear control problems. In this part, a sliding mode controller for attitude trajectory tracking control is developed. The laws presented in this part will be used directly in the position trajectory tracking controller design part.

Part of the state variable X is selected to form a new sub-state variable χ, and the considered attitude dynamic system can be extracted as follows:

$$\begin{cases} \dot{\chi}_1 = \chi_2 \\ \dot{\chi}_2 = a_1 \chi_4 \chi_6 + a_2 \varpi \chi_4 - a_3 \chi_2 + U_{S1} \\ \dot{\chi}_3 = \chi_4 \\ \dot{\chi}_4 = a_4 \chi_2 \chi_6 + a_5 \varpi \chi_2 - a_6 \chi_4 + U_{S2} \\ \dot{\chi}_5 = \chi_6 \\ \dot{\chi}_6 = a_7 \chi_2 \chi_4 - a_8 \chi_6 + U_{S3} \end{cases} \tag{11}$$

where $\chi = \left[\phi, \dot{\phi}, \theta, \dot{\theta}, \psi, \dot{\psi}\right]^T \in \Re^6$ and the parameters are same as the above mentioned ones in (9). Our control objective for the attitude system (11) is to ensure the trajectory tracking of $\{\phi(t),\theta(t),\psi(t)\}$ along the desired attitude trajectory $\{\phi_d(t),\theta_d(t),\psi_d(t)\}$ by designing SMC laws $U_S = \left[U_{S1}, U_{S2}, U_{S3}\right]^T$.

The regular sliding mode controller for attitude trajectory tracking control starts with the roll angle. A proper sliding manifold for roll motion control is chosen as follows:

$$s_1 = \dot{\varepsilon}_1 + c_1 \varepsilon_1 \tag{12}$$

where $\varepsilon_1 = \chi_{1d} - \chi_1$, c_1 is a positive constant and χ_{1d} is the desired roll angle command. The derivative of s_1 with respect to time is

$$\begin{aligned} \dot{s}_1 &= \ddot{\varepsilon}_1 + c_1 \dot{\varepsilon}_1 \\ &= \ddot{\chi}_{1d} - \ddot{\chi}_1 + c_1 \dot{\varepsilon}_1 \\ &= \ddot{\chi}_{1d} + c_1 \dot{\varepsilon}_1 - (a_1 \chi_4 \chi_6 + a_2 \varpi \chi_4 - a_3 \chi_2) - U_{S1} \\ &= \ddot{\chi}_{1d} + c_1 \dot{\chi}_{1d} - (a_1 \chi_4 \chi_6 + a_2 \varpi \chi_4 - a_3 \chi_2 - c_1 \chi_2) - U_{S1} \end{aligned} \tag{13}$$

where $\dot{\chi}_{1d}$ and $\ddot{\chi}_{1d}$ are the derivative and second derivative of the desired roll angle command which can be obtained approximately by stable first and second order differential filters. Assume that the state variables in (11) are measurable and the sliding mode control law for roll motion is designed as follows:

$$U_{S1} = \ddot{\chi}_{1d} + c_1 \dot{\varepsilon}_1 - (a_1 \chi_4 \chi_6 + a_2 \varpi \chi_4 - a_3 \chi_2) + k_1 sign(s_1) \tag{14}$$

where $sign(\cdot)$ is the sign function; k_1 is a positive constant to be determined and is also often in accordance to the requirement of performance and can be acquired through trial and error.

A Lyapunov canditate is chosen as follow:

$$V_{S1} = \frac{1}{2} s_1{}^2 \tag{15}$$

The derivative of (15) with respect to time can be written as (16) when U_{S1} is substituted.

$$\begin{aligned} \dot{V}_{S1} &= s_1 \dot{s}_1 \\ &= s_1 \left(\ddot{\chi}_{1d} + c_1 \dot{\varepsilon}_1 - (a_1 \chi_4 \chi_6 + a_2 \varpi \chi_4 - a_3 \chi_2) - U_{S1} \right) \\ &= -s_1 * k_1 sign(s_1) \\ &= -k_1 |s_1| \le 0 \end{aligned} \tag{16}$$

The combination of (15) and (16) implies that the sliding manifold designed in (12) is reachable.

This article has been accepted for publication in a future issue of this journal, but has not been fully edited. Content may change prior to final publication. Citation information: DOI 10.1109/TIE.2016.2552151, IEEE Transactions on Industrial Electronics

Similar design procedures can be conducted to design SMC laws for trajectory tracking control of pitch angle (χ_3) and yaw angle (χ_5). The corresponding control laws are designed as follows:

$$\begin{cases} U_{S2} = \ddot{\chi}_{3d} + c_2\dot{\varepsilon}_3 - (a_4\chi_2\chi_6 + a_5\varpi\chi_2 - a_6\chi_4) + k_2 sign(s_2) \\ U_{S3} = \ddot{\chi}_{3d} + c_3\dot{\varepsilon}_5 - (a_7\chi_2\chi_4 - a_8\chi_6) + k_3 sign(s_3) \end{cases} \quad (17)$$

where $s_2 = \dot{\varepsilon}_3 + c_2\varepsilon_3$ and $s_3 = \dot{\varepsilon}_5 + c_3\varepsilon_5$ are the properly designed sliding manifolds for pitch angle and yaw angle trajectory control. $\varepsilon_3 = \chi_{3d} - \chi_3$ and $\varepsilon_5 = \chi_{5d} - \chi_5$ are state errors. c_2 , c_3 , c_4 , k_2 , k_3 and k_4 are positive constants to be determined and need to be tuned by trial and error to reach the requirement of performance of the system.

The Lyapunov candidate for attitude system (11) is chosen as

$$V_S = \frac{1}{2}(s_1^2 + s_2^2 + s_3^2) \quad (18)$$

The derivative of (18) with respect to time can be written as (19) with U_{S1}, U_{S2}, U_{S3} being substituted by (14) and (17).

$$\begin{aligned} \dot{V}_S &= \sum_{i=1}^{3} s_i\dot{s}_i \\ &= \sum_{i=1}^{3} -s_i * k_i sign(s_i) \\ &= \sum_{i=1}^{3} -k_i|s_i| \le 0 \end{aligned} \quad (19)$$

Thus, the stability of the attitude system (11) is guaranteed by (18)-(19), ensuring attitude trajectory tracking capability.

In this part, regular SMC laws for attitude trajectory tracking control of a quadrotor UAV are presented. Sliding surfaces are chosen similarly for each Euler angle and control laws are designed under the assumption that state variables in (11) are measurable. Lyapunov-based analysis shows the stability of such an attitude subsystem. On the basis of the preceding regular SMC laws, a robust backstepping sliding mode controller for position trajectory tracking control is presented in the following part.

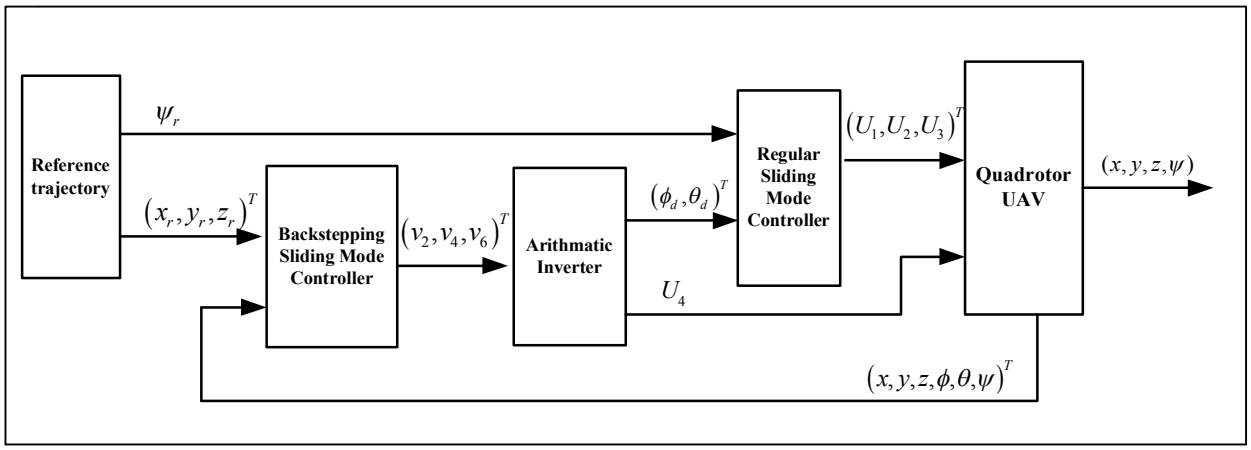

Fig.2 Block diagram of the control structure

B. Robust Backstepping Sliding Mode Control Design for Position Trajectory Tracking Control

The regular sliding mode controller for attitude control of a quadrotor UAV presented above is effective in terms of attitude trajectory tracking. It guarantees stability of the attitude subsystem and provides tracking capability. However, the controller has some deficiencies in realizing position control since that the dynamic model has an adverse form. In (9), control input U_4 is explicitly related to positions $\{x(t), y(t), z(t)\}$ and is the single external excitation for each of these three controlled variables. This means designing a separate sliding control law for each position variable is impossible. Thus, SMC alone is not suitable for position trajectory tracking control. This part presents a robust backstepping sliding mode controller based on the aforementioned regular sliding mode control law. The forthcoming controller is a combination of sliding mode control technique and backstepping control technique. On the one hand, backstepping control starts from Cartesian position trajectory tracking, utilizes virtual controls, stabilizes each subsystem and stops when the desired inner Euler angles are obtained. On the other hand, we apply the desired Euler angle commands to the attitude subsystem and obtain the final sliding mode control law. Thus, the proposed controller has advantages in both dealing with nonlinear system (a merit of backstepping control) and possessing robustness against model uncertainties and disturbances (the feature and advantage of sliding mode control). Our control objective with the proposed controller is to ensure that the position trajectory $\{x(t), y(t), z(t), \psi(t)\}$ converges to the reference trajectory $\{x_r(t), y_r(t), z_r(t), \psi_r(t)\}$. The control strategy adopted in this section is that the inner loop ($\phi(t), \theta(t), \psi(t)$) is controlled by sliding mode laws, and a fast convergence is ensured to the desired trajectory $\{\phi_d(t), \theta_d(t), \psi_d(t)\}$ while the outer loop ($x(t), y(t), z(t)$) is stabilized progressively until the ultimate backstepping control laws are obtained.

The backstepping sliding mode control design of position trajectory tracking control for system (9) starts with position x in the inertia frame. A sliding mode manifold $s_{p1} = v_1 - x_8$ is first introduced, where v_1 is a virtual control to be determined. The Lyapunov candidate chosen for this step is given by

$$V_1 = \frac{1}{2}z_7^2 \quad (20)$$

This article has been accepted for publication in a future issue of this journal, but has not been fully edited. Content may change prior to final publication. Citation information: DOI 10.1109/TIE.2016.2552151, IEEE Transactions on Industrial Electronics

where $z_7 = x_{7r} - x_7$ is the tracking error between reference position x_r and actual position x .The derivative of (20) with respect to time is given by

$$\dot{V}_1 = z_7\dot{z}_7 = z_7(\dot{x}_{7r} - x_8) = z_7(\dot{x}_{7r} - v_1 + s_{p1}) \tag{21}$$

To stabilize V_1 , the virtual control v_1 is designed as $v_1 = \dot{x}_{7r} + \rho_1 z_7$, where ρ_1 is a positive constant. By substituting it into (21), the following equation can be obtained

$$\dot{V}_1 = z_7\dot{z}_7 = z_7(-\rho_1 z_7 + s_{p1}) = -\rho_1 {z_7}^2 + z_7 s_{p1} \tag{22}$$

After v_1 is designed, the state error dynamics of z_7 can be obtained as follows:

$$\dot{z}_7 = -\rho_1 z_7 + s_{p1} \tag{23}$$

A second Lyapunov function involving state error z_7 is considered as follows:

$$V_2 = \frac{1}{2}({z_1}^2 + {s_{p1}}^2) \tag{24}$$

and a second virtual control $v_2 = (C_{x_1}S_{x_3}C_{x_5} + S_{x_1}S_{x_5})U_4$ is introduced. Up to now, as a control input, U_4 is still the one to be determined. The derivative of (24) with respect to time is then given by

$$\begin{aligned}\dot{V}_2 &= z_7\dot{z}_7 + s_{p1}\dot{s}_{p1}\\ &= z_7(-\rho_1 z_7 + s_{p1}) + s_{p1}(\dot{v}_1 - \dot{x}_8)\\ &= -\rho_1 {z_7}^2 + s_{p1}(z_7 + \dot{v}_1 - (C_{x_1}S_{x_3}C_{x_5} + S_{x_1}S_{x_5})U_4 + a_9 x_8)\\ &= -\rho_1 {z_7}^2 + s_{p1}(\dot{v}_1 + z_7 + a_9 x_8 - v_2)\end{aligned} \tag{25}$$

The stabilization of V_2 can be obtained by designing the virtual control as $v_2 = \dot{v}_1 + z_7 + a_9 x_8 + \rho_2 s_{p1}$. By substituting it into (25), the following inequality can be obtained.

$$\begin{aligned}\dot{V}_2 &= -\rho_1 {z_7}^2 + s_{p1}(\dot{v}_1 + z_7 + a_9 x_8 - v_2)\\ &= -\rho_1 {z_7}^2 - \rho_2 {s_{p1}}^2\\ &\le 0\end{aligned} \tag{26}$$

where ρ_2 is a positive constant.

For the trajectory tracking control of x_9 along with x_{9r} , a sliding manifold $s_{p2} = v_3 - x_{10}$ is introduced, where, v_3 is a virtual control to be determined to guarantee the tracking capability of x_9 along with x_{9r} . A Lyapunov candidate in this step is considered as

$$V_3 = \frac{1}{2}{z_9}^2 \tag{27}$$

where $z_9 = x_{9r} - x_9$ is the tracking error between reference position y_r and actual position y . The derivative of V_3 with respect to time is given by

$$\dot{V}_3 = z_9\dot{z}_9 = z_9(\dot{x}_{9r} - x_{10}) = z_9(\dot{x}_{9r} - v_3 + s_{p2}) \tag{28}$$

To stabilize V_3 , the virtual control v_3 is designed as $v_3 = \dot{x}_{9r} + \rho_3 z_9$, where ρ_3 is a positive constant. By substituting v_3 into (28), the following equation can be obtained:

$$\dot{V}_3 = z_9(\dot{x}_{9r} - v_3 + s_{p2}) = -\rho_3 {z_9}^2 + z_9 s_{p2} \tag{29}$$

Similar to (23), the state error dynamics is obtained as follows:

$$\dot{z}_9 = -\rho_3 z_9 + s_{p2} \tag{30}$$

A Lyapunov function involving the state error z_9 is chosen as

$$V_4 = \frac{1}{2}({z_7}^2 + {s_{p1}}^2 + {z_9}^2 + {s_{p2}}^2) \tag{31}$$

and a virtual control $v_4 = (C_{x_1}S_{x_3}S_{x_5} - S_{x_1}S_{x_5})U_4$ is introduced. Until now, U_4 is undtermined and need to be evaluated. The derivative of (31) with respect to time is

$$\begin{aligned}\dot{V}_4 &= z_7\dot{z}_7 + s_{p1}\dot{s}_{p1} + z_9\dot{z}_9 + s_{p2}\dot{s}_{p2}\\ &= \dot{V}_2 + z_9(-\rho_3 z_9 + s_{p2}) + s_2(\dot{v}_3 - \dot{x}_{10})\\ &= \dot{V}_2 - \rho_3 {z_9}^2 + s_{p2}(z_9 + \dot{v}_3 - (C_{x_1}S_{x_3}S_{x_5} - S_{x_1}S_{x_5})U_4 + a_{10}x_{10})\\ &= \dot{V}_2 - \rho_3 {z_9}^2 + s_{p2}(z_9 + \dot{v}_3 - v_4 + a_{10}x_{10})\end{aligned} \tag{32}$$

The stabilization of V_4 can be obtained by setting the virtual control as $v_4 = \dot{v}_3 + z_9 + a_{10}x_{10} + \rho_4 s_{p2}$, where ρ_4 is a positive constant. Then, (32) becomes

$$\begin{aligned}\dot{V}_4 &= \dot{V}_2 - \rho_3 {z_9}^2 + s_{p2}(z_9 + \dot{v}_3 - v_4 + a_{10}x_{10})\\ &= \dot{V}_2 - \rho_3 {z_9}^2 - \rho_4 {s_{p2}}^2 \le 0\end{aligned} \tag{33}$$

The backstepping procedure continues and a new sliding mode manifold is introduced as $s_{p3} = v_5 - x_{12}$, where v_5 is a virtual to be determined. At this step, the error measure is chosen as

$$V_5 = \frac{1}{2}{z_{11}}^2 \tag{34}$$

where $z_{11} = x_{11r} - x_{11}$ is tracking error between reference position z_r and actual position z . The derivative of (34) with respect to time is given by

$$\dot{V}_5 = z_{11}\dot{z}_{11} = z_{11}(\dot{x}_{11r} - x_{12}) = z_{11}(\dot{x}_{11r} - v_5 + s_{p3}) \tag{35}$$

To stabilize V_5 , the virtual control v_5 is designed as $v_5 = \dot{x}_{11r} + \rho_5 z_{11}$, where ρ_5 is a positive constant. By substituting v_5 into (35), the following equation can be obtained:

$$\dot{V}_5 = z_{11}(\dot{x}_{11r} - v_5 + s_{p3}) = -\rho_5 {z_{11}}^2 + z_{11}s_{p3} \tag{36}$$

Similar to (23), the tracking error dynamics are then obtained as follows:

$$\dot{z}_{11} = -\rho_5 z_{11} + s_3 \tag{37}$$

A Lyapunov function involving state error z_{11} is considered as

$$V_6 = \frac{1}{2}({z_7}^2 + {s_{p1}}^2 + {z_9}^2 + {s_{p2}}^2 + {z_{11}}^2 + {s_{p3}}^2) \tag{38}$$

and a virtual control $v_6 = (C_{x_1}C_{x_3})U_4$ is introduced where U_4 is unknown till now. The derivative of (38) with respect to time is given by

$$\begin{aligned}\dot{V}_6 &= z_7\dot{z}_7 + s_{p1}\dot{s}_{p1} + z_9\dot{z}_9 + s_{p2}\dot{s}_{p2} + z_{11}\dot{z}_{11} + s_{p3}\dot{s}_{p3}\\ &= \dot{V}_4 + z_{11}(-\rho_5 z_{11} + s_3) + s_3(\dot{v}_5 - \dot{x}_{12})\\ &= \dot{V}_4 - \rho_5 {z_{11}}^2 + s_3(z_{11} + \dot{v}_5 + g + a_{12}x_{12} - v_6)\end{aligned} \tag{39}$$

The stabilization of V_6 can be obtained by designing the virtual control as $v_6 = \dot{v}_5 + z_{11} + g + a_{11}x_{12} + \rho_6 s_{p3}$, where ρ_6 is a positive constant. Then, (39) becomes

$$\begin{aligned}\dot{V}_6 &= \dot{V}_4 + \dot{V}_5 + s_3(z_{11} + \dot{v}_5 + g + a_{12}x_{12} - v_6)\\ &= \dot{V}_4 - \rho_5 {z_{11}}^2 - \rho_6 {s_{p3}}^2 \le 0\end{aligned} \tag{40}$$

The combination of (38) and (40) indicates that the stability of the overall system is guaranteed and position trajectory tracking capability is ensured. Ultimate control laws are finally designed from the virtual controls introduced in these backstepping steps.

By associating v_2 , v_4 and v_6 , a group of virtual controls

This article has been accepted for publication in a future issue of this journal, but has not been fully edited. Content may change prior to final publication. Citation information: DOI 10.1109/TIE.2016.2552151, IEEE Transactions on Industrial Electronics

is obtained as:

$$\begin{aligned} v_2 &= (C_{x_1} S_{x_3} C_{x_5} + S_{x_1} S_{x_5}) U_4 \\ v_4 &= (C_{x_1} S_{x_3} S_{x_5} - S_{x_1} S_{x_5}) U_4 \\ v_6 &= (C_{x_1} C_{x_3}) U_4 \end{aligned} \tag{41}$$

Remark 3.1: v_2, v_4, and v_6 are combinations of available terms either by measuring or given directly as aforementioned. Thus, they can be regarded as known in the controlled system (11) and the control input U_4 can be solved.

Notably, equation (41) has 4 degrees of freedom, namely, x_1, x_3, x_5 and U_4. We also point out that a reference trajectory for yaw angle, i.e. x_{5r}, is usually given in advance as an extra reference signal and the corresponding SMC law U_3 is directly designed to ensure the rapid convergence of x_5 to x_{5r}. Thus, x_5 is regarded as known and can be replaced by x_{5r} in this case, and the degrees of freedom in (41) is reduced such that x_1, x_3, and U_4 can be solved. The solutions are as follows:

$$\begin{cases} x_{1d} = \arctan\left(\dfrac{\mathrm{ac}\, v_6 - d v_4}{a v_6 \sqrt{c^2 + d^2}} \right) \\ x_{3d} = \arctan\left(\dfrac{c}{d} \right) \\ U_4 = \dfrac{a^2(\mathrm{c}^2 + \mathrm{d}^2) v_6^{\,2} + (\mathrm{ac}\, v_6 - d v_4)^2}{ad} \end{cases} \tag{42}$$

where x_{1d} and x_{3d} are desired the roll angle trajectory and pitch angle trajectory for the inner loop, and U_4 is part of the ultimate control laws, and $a = \cos(x_{5r})$, $b = \sin(x_{5r})$, $c = (v_2 + v_4)/v_6$ and $d = a + b$.

Remark 3.2: According to Remark 2.1, it is trivial to point out that solutions in (42) are meaningful. In particular, the denominator of U_4 will not cause singularity since the yaw angle is limited to $(-\pi/2, \pi/2)$.

By taking $\{x_{1d}, x_{3d}, x_{5r}\}$ as desired attitude trajectory, the ultimate control laws can be obtained by applying the preceding SMC law design procedure and are presented as follows:

$$\begin{cases} U_1 = \ddot{x}_{1d} + c_1 \dot{z}_1 - (a_1 x_4 x_6 + a_2 \varpi x_4 - a_3 x_2) + k_1 sign(s_1(z_1)) \\ U_2 = \ddot{x}_{3d} + c_2 \dot{z}_3 - (a_4 x_2 x_6 + a_5 \varpi x_2 - a_6 x_4) + k_2 sign(s_2(z_3)) \\ U_3 = \ddot{x}_{5r} + c_3 \dot{z}_5 - (a_7 x_2 x_4 - a_8 x_6) + k_3 sign(s_3(z_5)) \end{cases} \tag{43}$$

where $s_i(z_{2i-1}) = \dot{z}_{2i-1} + c_{2i} z_{2i-1}$, $i = 1,2,3$ are the accordingly chosen sliding mode manifolds.

Ultimate control laws are finally obtained from (42) and (43) via the SMC and the backstepping control techniques. In addition, progressive stability analysis of the closed loop system guarantees the stability of the overall system (9) and ensures the position trajectory tracking capability of the proposed backstepping sliding mode controller.

IV. FAULT ESTIMATION FOR A QUADROTOR UAV

The presented backstepping sliding mode controller is a typical passive fault tolerant controller that handles disturbances and uncertainties well without knowing their information. This section investigates a method that estimates the fault information to complement our passive robust position trajectory tracking controller design. We know that the vertical taking off and the hovering mode are the common and important flight modes for a quadrotor UAV. And any fault, especially actuator fault, during the taking off phase may cause catastrophic consequence and even crash, resulting in great loss. Thus, we give a practical linear fault estimation module for the simplified model in taking off and hovering mode instead of a nonlinear one for the complicated complete dynamics. The fault estimation scheme will work as an alarming module and give a rough estimate of the occurring faults, indicating the changing trend and amplitude. Based on these estimates, a fault tolerant control algorithm may be developed. An adaptive observer based fault estimation is adopted for its fast implementation.

A multiple-input and multiple-output (MIMO) linear dynamic system with faults can be written as follows:

$$\begin{cases} \dot{x}(t) = Ax(t) + Bu(t) + Ef(t) \\ y = Cx(t) \end{cases} \tag{44}$$

where $x(t) \in \Re^n$ is the state variable vector, $u(t) \in \Re^m$ is the input vector, $y(t) \in \Re^p$ is the output vector, and $f(t) \in \Re^r$ is the fault. A, B, C, D are known matrices of dimension $n \times n, n \times m, p \times n, p \times m$. $E \in \Re^{n \times r}$ is fault distribution matrix.

In this part, a fault estimation scheme for system (44) is considered with the following assumptions.

Assumption 1: The fault is bounded and the derivative of the fault is bounded, that is

$$\|f(t)\| \le f_0, \quad \|\dot{f}(t)\| \le f_1 \tag{45}$$

where f_0 and f_1 are two positive scalars.

Remark 4.1: Assumption 1 is a little strict in light of that no priori knowledge about actual faults signal bound is known in real application. Yet, we know for sure that the upper bound of fault signal exists.

The fault estimation observer constructed for the faulty system (44) is given by

$$\begin{cases} \dot{\hat{x}}(t) = A\hat{x}(t) + Bu(t) + E\hat{f}(t) - L(\hat{y}(t) - y(t)) \\ \hat{y}(t) = C\hat{x}(t) \end{cases} \tag{46}$$

where $L \in \Re^{n \times p}$ is the observer gain matrix.

Equation (47) is defined as follows:

$$\begin{cases} e_x(t) = \hat{x}(t) - x(t) \\ e_y(t) = \hat{y}(t) - y(t) \\ e_f(t) = \hat{f}(t) - f(t) \end{cases} \tag{47}$$

Considering the derivative of (47) and the error dynamics is obtained as follows:

$$\begin{cases} \dot{e}_x(t) = (A - LC) e_x(t) + E e_f(t) \\ e_y(t) = C e_x(t) \end{cases} \tag{48}$$

The adaptive fault estimation algorithm is chosen as

$$\dot{\hat{f}}(t) = -\Gamma F e_y(t) \tag{49}$$

where $\Gamma > 0$ is the learning rate matrix and F is the matrix to be designed. Notably, such algorithm is only suitable for constant faults, that is $\dot{f}(t) = 0$.

The derivative of $e_f(t)$ with respect to time is given by

$$\dot{e}_f(t) = \dot{\hat{f}}(t) \tag{50}$$

THEOREM 4.1: If there exists a symmetric positive definite matrix $P \in \Re^{n \times n}$ and matrices $Y \in \Re^{n \times p}$, $F \in \Re^{r \times p}$ such that the following condition holds

This article has been accepted for publication in a future issue of this journal, but has not been fully edited. Content may change prior to final publication. Citation information: DOI 10.1109/TIE.2016.2552151, IEEE Transactions on Industrial Electronics

$$\begin{cases} PA + A^T P - YC - C^T Y^T < 0 \\ E^T P = FC \end{cases} \tag{51}$$

The fault estimation algorithm (49) then guarantees that the state error $e_x(t)$ and fault estimation error $e_f(t)$ converge to zero asymptotically. In this paper, the observer gain matrix is chosen as

$$L = P^{-1}Y \tag{52}$$

The proof of Theorem 1 is as follow.

Proof: Considering the Lyapunov candidate

$$V(t) = e_x^{\ T}(t)Pe_x(t) + e_f^{\ T}(t)\Gamma^{-1}e_f(t) \tag{53}$$

The derivative of $V(t)$ with respect to time is

$$\begin{aligned} \dot{V}(t) &= \dot{e}_x^{\ T}(t)Pe_x(t) + e_x^{\ T}(t)P\dot{e}_x(t) \\ &\quad + \dot{e}_f^{\ T}(t)\Gamma^{-1}e_f(t) + e_f^{\ T}(t)\Gamma^{-1}\dot{e}_f(t) \end{aligned} \tag{54}$$

Then, with the aid of (47), we have

$$\begin{aligned} \dot{V}(t) &= e_x^{\ T}(t)(P(A-LC) + (A-LC)^T P)e_x(t) \\ &\quad + 2e_x^{\ T}(t)PEe_f(t) - 2e_f^{\ T}(t)Fe_y(t) \\ &= e_x^{\ T}(t)(P(A-LC) + (A-LC)^T P)e_x(t) \\ &\quad + 2e_x^{\ T}(t)PEe_f(t) - 2e_f^{\ T}(t)FCe_x(t) \end{aligned} \tag{55}$$

By combining (50) and (55), the following equation is obtained:

$$\dot{V}(t) = e_x^{\ T}(t)(P(A-LC) + (A-LC)^T P)e_x(t) \tag{56}$$

Thus, if condition $PA + A^T P - YC - C^T Y^T < 0$ holds, he state estimation error $e_x(t)$ and fault estimation error $e_f(t)$ converge to zero asymptotically. The proof for Theorem 4.1 is completed. This fault estimation scheme is used in vertical taking off and landing phase to avoid crash landing by estimating the faults rapidly.

V. SIMULATION

In this section, simulations are conducted to verify the effectiveness of the presented robust backstepping sliding mode controller and adaptive observer based fault estimation. Different scenarios are considered, including normal case, cases under model undertainty and external disturbances, and even the case under Gaussian white noise, to demonstrate the robustmess of the proposed controller. The nominal parameters for the quadrotor UAV adopted in this study are same as those described in Table 1 [2, 12].

A. Simulation for Backstepping Sliding Mode Controller

The effectiveness of the proposed backstepping sliding mode controller is verified by comparing the position trajectory tracking performance in normal case and in cases with uncertain parameters and even with white Gaussian noise. The desired trajectory of the position and yaw angle $\{x_r(t), y_r(t), z_r(t), \psi_r(t)\}$ in the simulation study is chosen as $\{\cos(t), \sin(t), 0.5t, \sin(0.5t)\}$. One thing should be noted is that the parameters in the robust controller design procedure ($\rho_i, i = 1,2,3,4,5,6$) should be tuned carefully given that these sliding mode surfaces. Therefore, these parameters affect the performance of the presented controller. To demonstrate the effectiveness of the developed robust controller, the following different scenarios are considered in the simulations and brief comparisons are conducted.

TABLE 1 QUADROTOR PARAMETERS

symbol	case 1	case 2	case 3	units
m	2	2	2	kg
l	0.2	0.2	0.2	m
κ	2.98	2.98	2.98	$10^{-6}Ns^2rad^{-2}$
τ	1.14	1.14	1.14	$10^{-7}Ns^2rad^{-2}$
d_ϕ	1.2	1.2	1.2	$10^{-2}Nsrad^{-1}$
d_θ, d_ψ	1.2	1.2	1.2	$10^{-2}Nsrad^{-1}$
J_x	1.25	0.94	1.25	Ns^2rad^{-1}
J_y	1.25	0.94	1.25	Ns^2rad^{-1}
J_z	2.50	1.88	3.63	Ns^2rad^{-1}

Scenario I：Normal case

In this case, we assume that the parameters of the quadrotor vehicle are normal, and neither the model uncertainty nor the disturbance is considered. Simulations for different initial states are conducted.

Scenario II：Uncertainty (25% subtracted) in rotary inertia

In this case, we consider model uncertainty 25% subtracted in all three body-frame axes. We also conduct simulations with the proposed controller and the existing backstepping controller in the same situations to compare their robustness against model uncertainties.

Scenario III: Uncertainty (%45 added) in rotary inertia as well the presence of external disturbance

In this case, we give a consideration to both uncertainty in rotary inertia and external disturbance. The uncertainty in yaw axis is 45% more and the disturbance is band-limited white noise of which the power is 0.005 and the sample time is 0.01 and the amplitude is limited to 0.3.

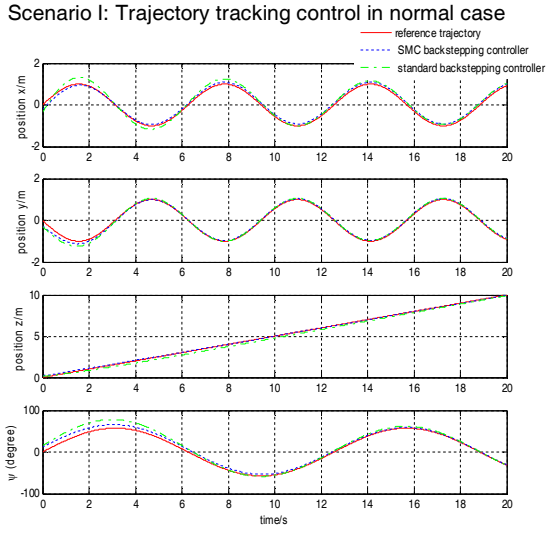

Fig.3 Normal case (red: reference trajectory, blue: SMC bacstepping controller, green: standard backstepping controller)

This article has been accepted for publication in a future issue of this journal, but has not been fully edited. Content may change prior to final publication. Citation information: DOI 10.1109/TIE.2016.2552151, IEEE Transactions on Industrial Electronics

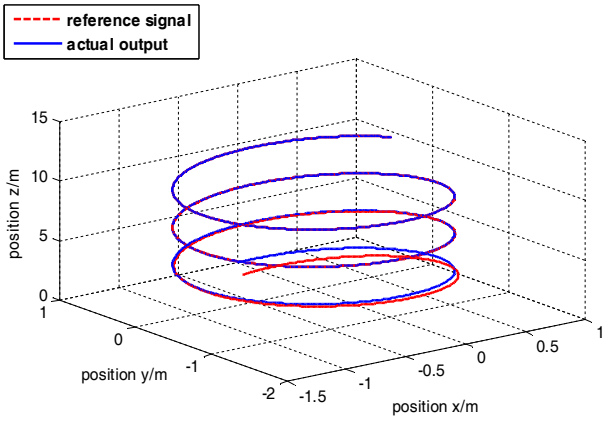

Fig. 4 Space diagram of position in normal case

Scenario II: Trajectory tracking control with uncertainty (25% subtracted) in rotary inertia

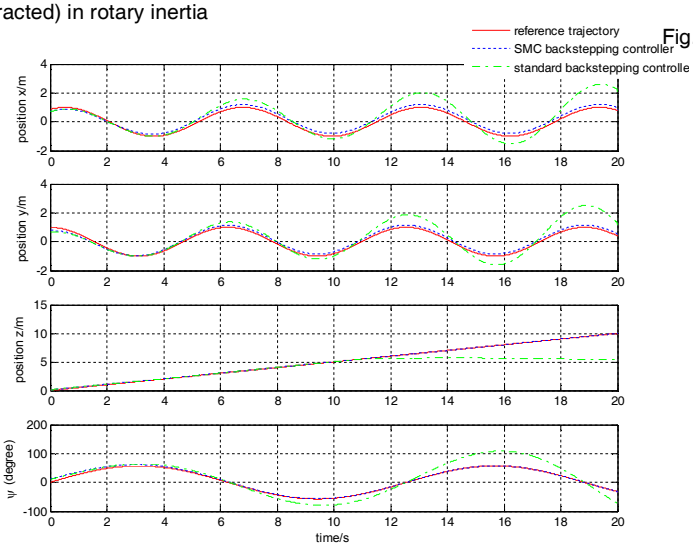

Fig. 5-(a) Uncertainty 25% subtracted in all three axes

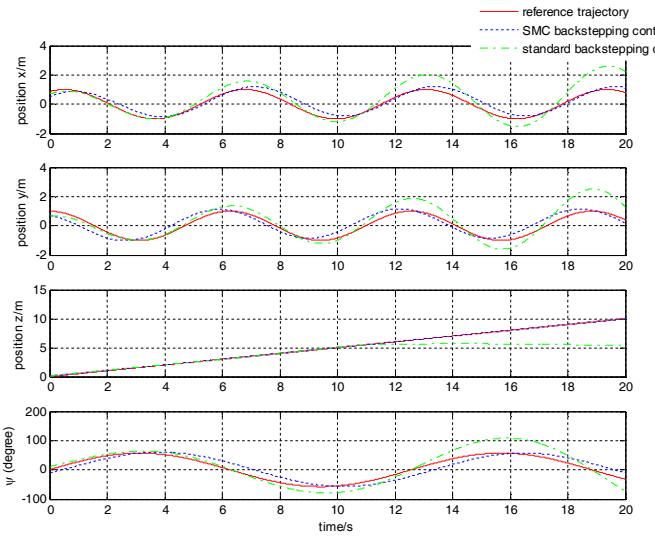

Fig. 5-(b) Uncertainty 25% subtracted in all three axes with filtered control signals

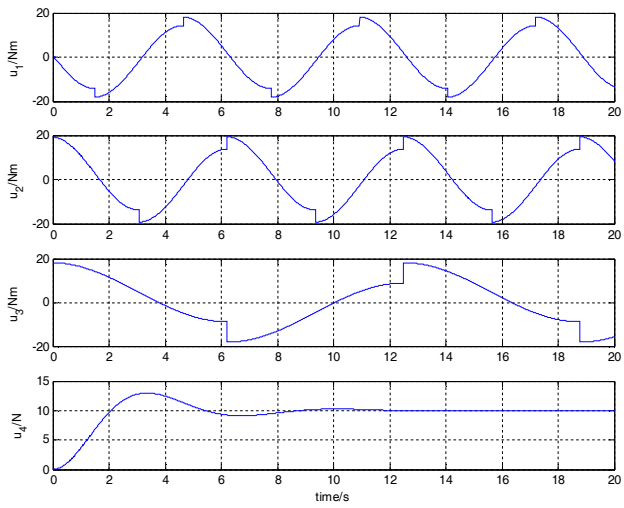

Fig. 5-(c) Control signals

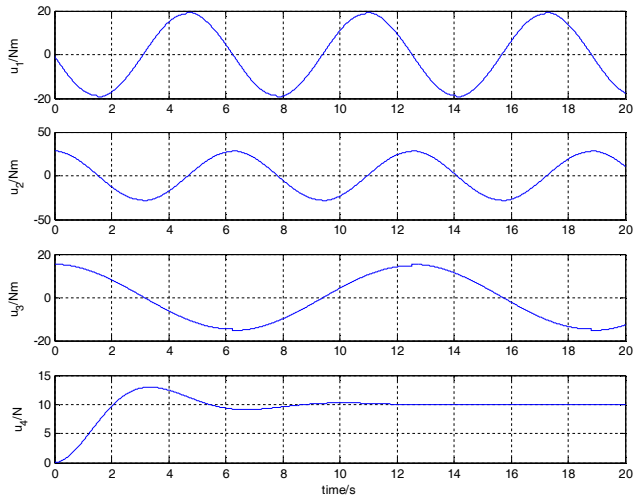

Fig. 5-(d) Filtered control signals

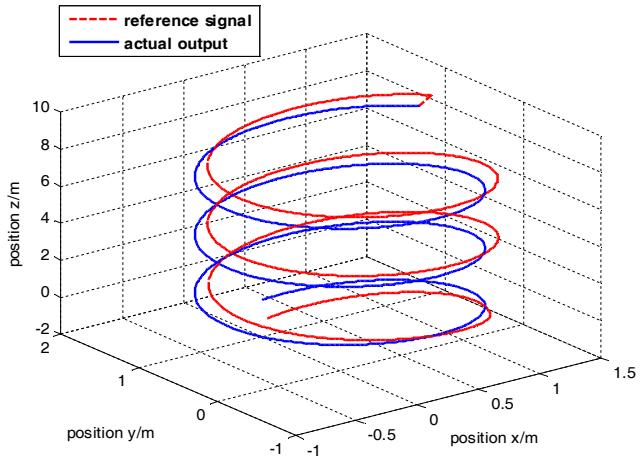

Fig. 6 Space diagram of position with uncertainty

This article has been accepted for publication in a future issue of this journal, but has not been fully edited. Content may change prior to final publication. Citation information: DOI 10.1109/TIE.2016.2552151, IEEE Transactions on Industrial Electronics

Scenario III: Trajectory tracking control with uncertainty (45% added) and white noise

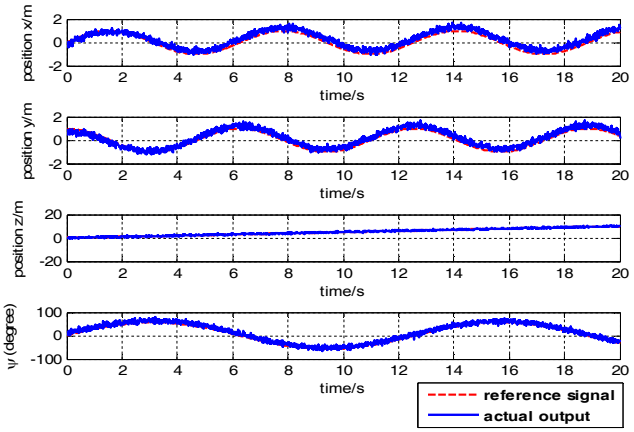

Fig. 7 Uncertainty 45% added in one rotating axis

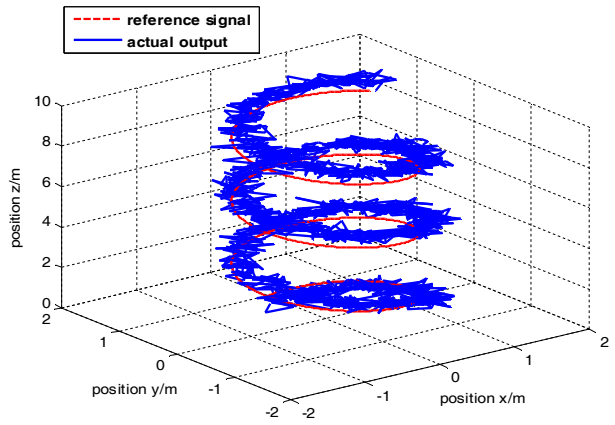

Fig. 8 Space diagram of position with uncertainty and white Gaussian noise

The position and yaw angle trajectories in Figs. 3 and 4 show satisfactory performances, that is, trajectory tracking is achieved in a few seconds. Moreover, we can see from Fig.3 that both standard backstepping controller and the proposed SMC backstepping controller work well in a normal case in terms of convergence rapidity and tracking error. Fig.5 (a)-(b) show the simulation results with standard and SMC backstepping controllers in an initial state different from normal case. Compared with Fig.5 (a), Fig.5 (b) shows a minor delay effect caused by the filtered control signal with a first order filter. Both 5(a) and 5(b) show that standard backstepping controller fails to handle such a case with uncertainty 25% subtracted in all three axes while the proposed controller succeeds in dealing with this case. Fig.5 (c) and Fig.5 (d) show the unfiltered control signals and the filtered ones by 8/(s+8). Figs. 7 and 8 illustrate the simulation results of the quadrotor system in scenarios which are under 45% uncertainty added in one of the three rotating axes in the presence of white Gaussian noise. From Fig.7 we can see that the proposed controller possesses trajectory tracking capability even under circumstances in which uncertainty in rotary inertia is up to 45% along with white noise at the same time. From Fig. 3 to Fig. 8, we can conclude that the proposed controller is robust to uncertainty of different levels and even with white noise simultaneously. The trajectory tracking performances in these simulations demonstrate the effectiveness of the robust controller against adverse condition.

B. Simulation for Fault Estimation Scheme

The vertical take-off phase of a quadrotor UAV is considered to verify the effectiveness of the adaptive observer based fault estimation scheme. The dynamic model represented by (6) and (7) can be simplified in this case. The take-off manipulation is assumed to be obtained by increasing the rotor speeds with identical quantity which means $\Omega_i, i=1,2,3,4$ have the identical quantity. Thus, the control inputs $U_i, i=1,2,3$ in (11) are zeros. U_4 is bound to be positive enough to overcome the mass of the quadrotor. Another assumption is that the initial states of the attitude angles and their derivatives with respect to time are all zeros, and this often makes sense. Under the preceeding assumptions, the taking off dynamic model is reduced to

$$\begin{cases} \dot{x}_{11} = x_{12} \\ \dot{x}_{12} = -g + (C_{x_1} C_{x_3}) U_4 - a_{11} x_{12} \end{cases} \tag{57}$$

which can be rewritten as a typical linear second-order system in the assumption that $C_{x1} = C_{x3} = 1$, which means the roll angle and the pitch angle are near zeros. The second order dynamics is

$$\ddot{z} = U_4 - g - d_z \dot{z} / m \tag{58}$$

where $z = x_{11}$ is the state variable. Thus, the aforementioned adaptive fault estimation method can be applied to estimate the fault information in this dynamic system.

Denote $z_1 = z$, $\dot{z}_1 = z_2$, $U = U_4 - g$, and consider possible actuator fault, the dynamic system becomes

$$\begin{aligned} \begin{bmatrix} \dot{z}_1 \\ \dot{z}_2 \end{bmatrix} &= \begin{bmatrix} 0 & 1 \\ -d_z / m & 0 \end{bmatrix} \begin{bmatrix} z_1 \\ z_2 \end{bmatrix} + \begin{bmatrix} 0 \\ 1 \end{bmatrix} u + \begin{bmatrix} 1 & 0 \\ 0 & 1 \end{bmatrix} \begin{bmatrix} 0 \\ f_1(t) \end{bmatrix} \\ &= \begin{bmatrix} 0 & 1 \\ -0.005 & 0 \end{bmatrix} \begin{bmatrix} z_1 \\ z_2 \end{bmatrix} + \begin{bmatrix} 0 \\ 1 \end{bmatrix} (u + f_1) \end{aligned} \tag{59}$$

$$w = \begin{bmatrix} 1 & 0 \\ 0 & 1 \end{bmatrix} \begin{bmatrix} z_1 \\ z_2 \end{bmatrix} \tag{60}$$

where w is output.

The parameters given in Theorem 1 can be obtained through LMI toolbox in MATLAB. The corresponding observer gain matrix L and the corresponding F is solved as

$$L = \begin{bmatrix} 0.5000 & -22.5519 \\ 23.5469 & 0.5000 \end{bmatrix}, F = \begin{bmatrix} 0 & 1 \end{bmatrix} \tag{61}$$

Simulations are conducted with these parameters and the results for fault estimation are shown in the following figures.

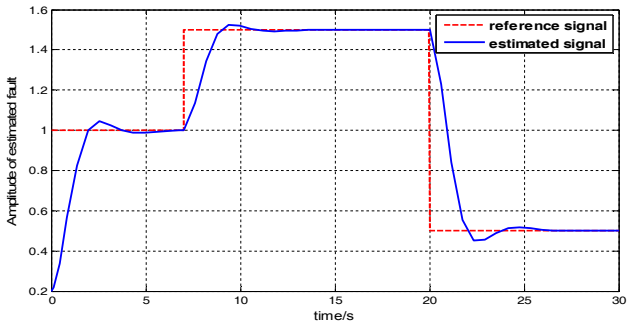

Fig. 9 Estimation of invariant fault

This article has been accepted for publication in a future issue of this journal, but has not been fully edited. Content may change prior to final publication. Citation information: DOI 10.1109/TIE.2016.2552151, IEEE Transactions on Industrial Electronics

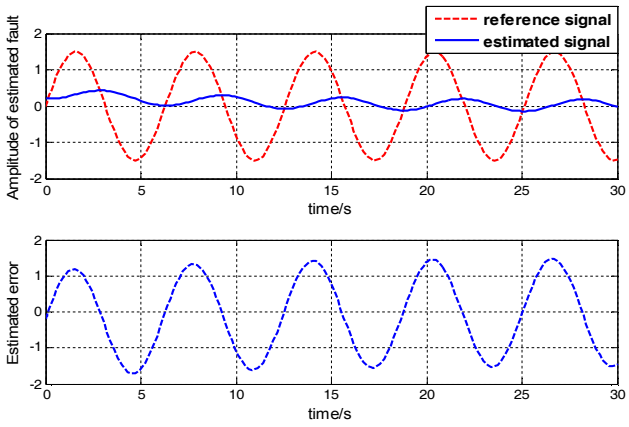

Fig. 10 Estimation of time-varying fault and estimation error

Fig. 9 shows the simulation result of employing adaptiveobserver to estimate the invariant fault signal

$$f_1(t)=\begin{cases}1; & t<7(\text{sec})\\ 1.5; & t\geq 7(\text{sec})\\ 0.5; & t>20(\text{sec})\end{cases}.$$

It is clear that the adaptive observer can estimate the invariant fault signal satisfyingly. Fig. 10 shows the simulation result of the system with a fault as $f(t)=1.5\sin(t)$, and the estimation error response illustrates that this fault estimation method fails to deal with time-varying faults.

Ⅵ. CONCLUSIONS

In this paper, we first present a regular sliding mode controller design for attitude control of a quadrotor UAV. On the basis of this design, we combineSMC technique and backstepping control technique to design a robust backstepping sliding mode controller for position and yaw angle control. Virtual control inputs are introduced in the robust controller design to guarantee the trajectory tracking performance. Sliding manifolds are designed to drive the actual variables to approximate the virtual ones. We present the stability analysis of the overall system through Lyapunov stability theory. Fault estimation is also considered in this study and is applied to the take-off phase of a quadrotor. The simulation results show that, robustness and improved tracking performance can be achieved with the proposed robust sliding mode controller. The simulation results also demonstrate the effectiveness of the presented fault estimation method. Our future works includes considering actuator fault and developing an active fault-tolerant controller based on the control design and fault estimation scheme proposed in this paper.

REFERENCES

[1] A. Tayebi, S. McGilvray, "Attitude stabilization of a VTOL quadrotor aircraft," *IEEE Trans. Contr. Syst. T.*, vol. 14, no. 3, pp.562-571, May, 2006.

[2] Z. Zuo, "Trajectory tracking control design with command-filtered compensation for a quadrotor," *IET Control Theory A.*, vol. 4, no. 11, pp. 2343-2355, Jan, 2010.

[3] P. E. I. Pounds, D. R. Bersak, A. M. Dollar, "Stability of small-scale UAV helicopters and quadrotors with added payload mass under PID control," *Auton. Robot.*, vol. 33, no. 1-2, pp. 129-142, Aug, 2012.

[4] A. Das, K. Subbarao, F. Lewis, "Dynamic inversion with zero-dynamics stabilisation for quadrotor control," *IET Control Theory A.*, vol. 3, no. 3, pp. 303-314, 2009.

[5] A. Mokhtari, A. Benallegue, Y. Orlov, "Exact linearization and sliding mode observer for a quadrotor unmanned aerial vehicle," *Int. J. Robot. Autom.*, vol. 21, no. 1, pp. 39-49, 2006.

[6] D. Lee, H. J. Kim, S. Sastry, "Feedback linearization vs. adaptive sliding mode control for a quadrotor helicopter," *Int. J. Contr. Auto.*, vol. 7, no. 3, pp. 419-428, Jun, 2009.

[7] K. Alexis, G. Nikolakopoulos, A. Tzes, "Model predictive quadrotor control: attitude, altitude and position experimental studies," *IET Contr. Theor. App.*, vol. 6, no. 12, pp. 1812-1827, Aug, 2012.

[8] C. H. Lin, S. S. Jan, F. B. Hsiao, "Autonomous hovering of an experimental unmanned helicopter system with proportional-integral sliding mode control," *J. Aerospace Eng.*, vol. 24, no. 3, pp. 338-348, Jul, 2010.

[9] A. Das, F. Lewis, K. Subbarao, "Backstepping approach for controlling a quadrotor using lagrange form dynamics," *J. Intell. Robot. Syst.*, vol. 56, no. 1-2, pp. 127-151, Sep, 2009.

[10] A. R. Merheb, H. Noura, F. Bateman, "Design of Passive Fault–Tolerant Controllers of a Quadrotor Based on Sliding Mode Theory," *Int. J. Appl. Math. Comput. Sci.*, vol. 25, no.3, pp. 561-576, 2015.

[11] T. Wang, W. F. Xie., Y. M. Zhang, "Sliding Mode Reconfigurable Control Using Information on the Control Effectiveness of Actuators," *J. Aerospace Eng.*, vol. 27, no. 3, pp. 587-596, May, 2014.

[12] T. Ryan, H. J. Kim, "LMI-based gain synthesis for simple robust quadrotor control," *IEEE Trans. Autom. Sci. Eng.*, vol. 10, no. 4, pp. 1173-1178, 2013.

[13] M. Kerma, A. Mokhtari, B. Abdelaziz, Y. Orlov, "Nonlinear H-infinity Control of a Quadrotor (UAV), Using High Order Sliding Mode Estimator," *Int. J. Contr.*, vol. 85, no. 12, pp. 1876-1885, 2012.

[14] L. Besnard, Y. B. Shtessel, B. Landrum, "Quadrotor vehicle control via sliding mode controller driven by sliding mode disturbance observer," *J. Franklin I.*, vol.349, no. 2, pp. 658-684, Mar, 2012.

[15] A. Benallegue, A. Mokhtari, L. Fridman, "High order sliding mode observer for a quadrotor UAV," *Int. J. Robust and Nonlin.*, vol. 18, no. 4-5, pp. 427-440, Mar, 2008.

[16] X. Wang, B. Shirinzadeh, M. H. Ang, "Nonlinear double-integral observer and application to quadrotor aircraft," *IEEE Trans. Ind. Electron.*, vol. 62, no. 2, pp. 1189-1200, Feb, 2015.

[17] R. C. Leishman, J. C. Macdonald, R. W. Beard, "Quadrotors and accelerometers: State estimation with an improved dynamic model," *IEEE Contr. Syst.*, vol. 34, no. 1, pp. 28-41, Feb, 2014.

[18] K. Lee, J. Back, I. Choy, "Nonlinear disturbance observer based robust attitude tracking controller for quadrotor UAVs," *Int. J. Contr. Autom.*, vol. 12, no. 6, pp. 1266-1275, Nov, 2014.

[19] X. J. Chen., D. Li., Y. Bai, "Modelling and Nero-Fuzzy Adaptive Control for Eight-Rotor MAV," *Int. J. Contr. Autom.*, vol. 9, no. 6, pp. 1154-1163, 2011.

[20] T. Lee, "Robust Adaptive Attitude Tracking on With an Application to a Quadrotor UAV," *IEEE Trans. Contr. Syst. T.*, vol. 21, no. 5, pp. 1924-1930, Sep, 2013.

[21] Z. T. Dydek, A. M. Annaswamy, E. Lavretsky, "Adaptive control of quadrotor UAVs: A design trade study with flight evaluations," *IEEE Trans. Contr. Syst. T.*, vol. 21, no. 4, pp. 1400-1406, 2013.

[22] X. Wang, B. Shirinzadeh, M. H. Ang, "Nonlinear double-integral observer and application to quadrotor aircraft," *IEEE Trans. Ind. Electron.*, vol. 62, no. 2, pp. 189-200, Feb, 2015.

[23] L. Wang, J. Su, "Robust Disturbance Rejection Control for Attitude Tracking of an Aircraft," *IEEE Trans. Contr. Syst. T.*, vol.23, no.6, pp.2361-2368, 2015.

[24] B. Erginer, E. Altuğ, "Design and implementation of a hybrid fuzzy logic controller for a quadrotor VTOL vehicle," *Int. J. Contr. Autom.*, vol. 10, no. 1, pp. 61-70, Feb, 2012.

[25] Y. Wang, Q. Wu, Y. Wang, "Consensus algorithm for multiple quadrotor systems under fixed and switching topologies," *Syst. Eng. and Electron.*, Journal of, vol. 24, no. 5, pp. 818-827, 2013.

[26] G. Nikolakopoulos, K. Alexis, "Switching networked attitude control of an unmanned quadrotor," *Int. J. Contr. Automa.*, vol. 11, no. 2, pp. 389-397, April, 2013.

[27] H. Liu, Y. Bai, G. Lu, Z. Shi, Y. Zhong, "Robust tracking control of a quadrotor helicopter," *J. Intell. Robot. Syst.*, vol. 75, no. 3-4, pp. 595-608, Sep, 2014.

[28] A. Chamseddine, D. Theilliol, Y. M. Zhang, C. Join, C. A. Rabbath, "Active fault tolerant control system design with trajectory replanning against actuator faults and saturation: Application to a quadrotor unmanned aerial vehicle," *Int. J. of Adapt. Control*, vol. 29, no. 1, pp. 1-23, 2014.

[29] H. Liu, G. Lu, Y. Zhong, "Robust LQR attitude control of a 3-DOF laboratory helicopter for aggressive maneuvers," *IEEE Trans. Ind. Electron.*, vol. 60, no. 10, pp. 4627-4636, Jan, 2013.

[30] S. Islam, P. X. Liu, A. El Saddik, "Robust Control of Four Rotor Unmanned Aerial Vehicles with Disturbance Uncertainty," *IEEE Trans. Ind. Electron.*, vol. 62, no. 3, pp. 1563-1571, Mar, 2014.

[31] H. Liu, J. Xi, Y. Zhong, "Robust motion control of quadrotors," *J. Franklin I.*, 2014, vol. 351, no. 12, pp. 5494-5510, Dec, 2014.
[32] A. Nasiri, S. K.Nguang, A. Swain, "Adaptive sliding mode control for a class of MIMO nonlinear systems with uncertainties," *J. Franklin I.*, vol. 351, no. 4, pp. 2048-2061, Jan, 2014.
[33] J. E. Slotine, "Sliding controller design for non-linear systems," *Int. J. Contr.*, vol. 40, no. 2, pp. 421-434, Aug, 1984.
[34] Y. Zhang, J. Jiang, "Bibliographical review on reconfigurable fault-tolerant control systems," *Ann. Rev. Contr.*, vol. 32, no. 2, pp. 229-252, Dec, 2008.
[35] K. Zhang, B. Jiang and P. Shi, "Fast fault estimation and accommodation for dynamical systems," *IET Contr. Theor. App.*, vol. 3, no. 2, pp.189-199, 2009.
[36] J. Liu, S. Laghrouche, M. Harmouche, "Adaptive-gain second-order sliding mode observer design for switching power converters," *Contr. Eng. Pract.*, vol. 30, pp.124-131, 2014.
[37] J. Liu, S. Laghrouche, M. Wack, "Observer-based higher order sliding mode control of power factor in three-phase AC/DC converter for hybrid electric vehicle applications, " *Int. J. Contr.*, vol. 87, no. 6, pp. 1117-1130, 2014.
[38] S. Laghrouche, J. Liu, F. S. Ahmed, "Adaptive second-order sliding mode observer-based fault reconstruction for pem fuel cell air-feed system," *IEEE Trans. Contr. Syst. T.*, vol. 23, no. 3, pp.1098-1109, 2015.
[39] S. Yin, X. Zhu, O. Kaynak, "Improved PLS focused on key-performance-indicator-related fault diagnosis," *IEEE Trans. Ind. Electron.*, vol. 62, no. 3, pp. 1651-1658, ,2015.
[40] S. Yin, S. X. Ding and X. Xie, "A review on basic data-driven approaches for industrial process monitoring," *IEEE Trans. Ind. Electron.*, vol. 61, no. 11, pp.6418-6428, 2014.
[41] S. Yin, X. Li, H. Gao, "Data-based techniques focused on modern industry: an overview," *IEEE Trans. Ind. Electron.*, vol. 62, no. 1, pp. 657-667, 2015.

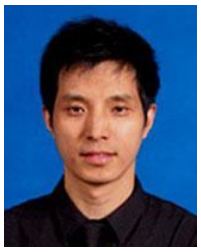

Fuyang Chen received the D.E. degree in Automation Engineering with the Nanjing University of Aeronautics and Astronautics, Nanjing, China in 2013. His research interests include adaptive control, flight control, quantum control and self-repairing control.

Rongqiang Jiang received his B.E. degree in Automation Engineering from Nanjing University of Post and Telecommunication in 2014. Now he is a master student at the Department of Automation, NUAA. His research interests include adaptive control, failure detection and fault-tolerant control.

Kangkang Zhang received his B.E. degree in Control Technology and Instruments from Xi'an University of Post and Telecommunication in 2013. Now he is a master student at the Department of Automation, NUAA. His research interests include aircraft modeling, adaptive control, failure detection and fault-tolerant control..

Bin Jiang (SM'05) was born in Jiangxi, China, in 1966. He received the Ph.D. degree in automatic control from Northeastern University, Shenyang, China, in 1995.

Dr. Jiang is the Chair of the Control Systems Chapter in the IEEE Nanjing Section and a member of the International Federation of Automatic Control (IFAC) Technical Committee on Fault Detection, Supervision, and Safety of Technical Processes. He currently serves as Associate Editor or Editorial Board Member for a number of journals such as the IEEE TRANSACTIONS ON CONTROL SYSTEMS TECHNOLOGY; *International Journal of Control, Automation and Systems*; *Nonlinear Analysis: Hybrid Systems*; *International Journal of Applied Mathematics and Computer Science*; *Acta Automatica Sinica*; and *Journal of Astronautics*.

Gang Tao (F'07) received the B.S. degree in electrical engineering from the University of Science and Technology of China, Hefei, China, in 1982, and the M.S. degrees in electrical engineering, computer engineering, and applied mathematics in 1984, 1987, and 1989, respectively, and the Ph.D. degree in electrical engineering from the University of Southern California, Los Angeles, in 1989.

He was a Visiting Professor with the Nanjing University of Aeronautics and Astronautics, Nanjing, China.His research interests include adaptive control of systems with uncertain actuator nonlinearities and failures, structural damage and sensor uncertainties, and aircraft flight control applications.